Some properties of the boundary over distance preconditioner for radial basis function interpolation

C. T. Mouat and R. K. Beatson

Department of Mathematics & Statistics,
University of Canterbury,
Private Bag 4800, Christchurch, New Zealand.

Report Number: UCDMS2001/6 July 2001

Keywords: radial basis functions, precondition, voronoi.

Some properties of the boundary over distance preconditioner for radial basis function interpolation

C. T. Mouat and R. K. Beatson

Department of Mathematics and Statistics
University of Canterbury
Christchurch, New Zealand

July 9, 2001

Abstract

In this paper we consider the boundary over distance preconditioner for radial basis function interpolation problems. We give both theoretical and numerical results indicating that it performs extremely well.

Keywords: radial basis functions, precondition, voronoi.

1 Introduction

Let $\Phi : \mathcal{R}^d \to \mathcal{R}$, $X = \{x_1, \ldots, x_N\}$ be a set of N distinct points in $\mathcal{R}^d$ and f be a real valued function which we can evaluate at least at the x_i's. Define

$$S_{\Phi,X} = \left\{ \begin{array}{l} g : g = \sum_{i=1}^{N} \lambda_i \Phi(\cdot - x_i) \\ \qquad \text{where } \sum_{j=1}^{N} \lambda_j q(x_j) = 0, \quad \text{for all } q \in \pi_1^d \end{array} \right\}. \tag{1}$$

We consider the problem of finding an element s of $S_{\Phi,X} + \pi_1^d$ satisfying the interpolation conditions

$$s(x_i) = f(x_i), \quad \text{for all} \quad x_i \in X. \tag{2}$$

Assume Φ is strictly conditionally positive definite of order 2 and X is unisolvent for π_1^d. Then there is a unique element of $S_{\Phi,X} + \pi_1^d$ satisfying the interpolation conditions (2). This setting includes popular choices of the basic function such as the thin-plate spline, $\Phi(\cdot) = |\cdot|^2 \log |\cdot|$, and minus the ordinary multiquadric, $\Phi(\cdot) = -\sqrt{|\cdot|^2 + c^2}$. In this paper we consider various ways of formulating the interpolation problem, showing in particular that a certain inexpensive change of basis can dramatically improve its conditioning.

The usual way to formulate this problem is in terms of the functions $\{\Phi(\cdot - x_i)\}$ and some basis $\{p_0, p_1, \ldots, p_d\}$ for π_1^d. Then the interpolation conditions together with the side conditions taking away the extra degrees of freedom introduced by the polynomial part can be written as

$$A\lambda + Pc = f \qquad \text{and} \qquad P^T\lambda = 0, \tag{3}$$

where

$$A_{ij} = \Phi(x_i - x_j), \qquad P_{ij} = p_j(x_i),$$

and $f = [f(x_1), \ldots, f(x_N)]^T$. It is well known [7, 10, 12] that the matrix

$$A_\Phi = \begin{bmatrix} A & P \\ P^T & O \end{bmatrix}, \tag{4}$$

of this usual formulation is frequently badly conditioned, even when the number of nodes is small. Indeed many authors have commented on the numerical difficulties that solving this system presents [12, 8, 7, 10]. However, frequently in numerical analysis a change of basis, or other reformulation, can make a highly intractable problem tractable. Indeed, in the case of the RBF interpolation equations changing to the basis of cardinal functions would result in the interpolation matrix becoming the identity and the system being perfectly conditioned and trivial to solve. Unfortunately, finding the cardinal RBFs would be more computationally expensive than solving the system itself. Hence, our goal is to find less expensive but still highly effective preconditioners for the interpolation system.

In this paper we establish properties of a preconditioning method for the RBF interpolation equations which was first presented in Sibson and Stone [12]. In the following section we give a detailed account of the preconditioning method. In Section 3 we prove that the construction produces a symmetric positive definite matrix B whenever the nodes X are unisolvent for π_1^2. In Section 4 we show that for certain functions Φ, B is a homogeneous function of scale. Hence, its condition number, and the relative clustering of its eigenvalues, are independent of scale. Section 5 contains a proof that the elements B_{ij} decay like $|x_i - x_j|^{-\kappa}$ when $|x_i - x_j|$ is large. For the multiquadric κ is three and for the thin-plate spline κ is two. Sections 6 and 7 contain numerical results for different SCPD2 basic functions over a range of data sets and scales. These numerical results show that using this inexpensive $\mathcal{O}(N \log N)$ flop preconditioner and variants of it, dramatically improves the conditioning of RBF interpolation problems. See Figure 1 below. Finally, Section 8 discusses the effects of roundoff error when using a fast technique to compute the product of the preconditioned matrix and a vector.

2 A preconditioning method

A general approach to preconditioning interpolation problems with SCPD2 basic functions in $\mathcal{R}^2$ [12, 1] is to choose Q as any $N \times (N-3)$ matrix whose columns are orthogonal to P

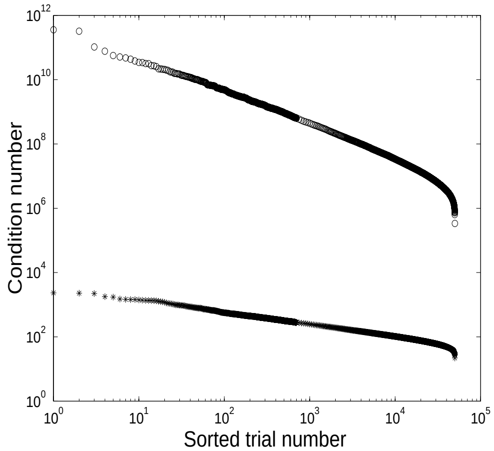

(a) Multiquadric basic function.

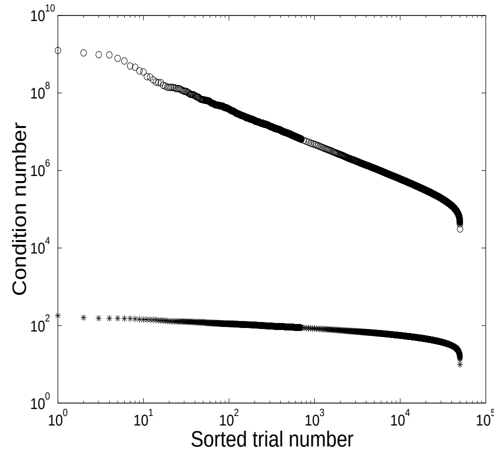

(b) Thin-plate spline basic function.

Figure 1: Sorted 2-norm condition numbers of the unpreconditioned matrices, A_Φ, (top) and of the preconditioned matrices, S, (bottom) for fifty thousand random data sets of size one hundred.

and has rank $N-3$. Letting $\lambda = Q\mu$ and premultiplying (3) by Q^T gives the new system to be solved for μ, or equivalently λ,

$$B\mu = Q^T f \qquad \text{where} \qquad B = Q^T A Q. \tag{5}$$

The three polynomial coefficients can then be found by a small subsidiary calculation. Note that we can view the jth column of the product AQ as the values of the corresponding new basis element,

$$\Psi_j(\cdot) = \sum_{i=1}^{N} q_{ij} \Phi(\cdot - x_i).$$

For the multiquadric and the thin-plate spline these Ψ elements have r^{-1} and $\log r$ growth respectively as r gets large. This can be seen in Figures 2 and 3 below.

The construction presented in this section produces a matrix Q such that B is positive definite for any set of distinct nodes $X = \{x_1, \ldots, x_N\} \subset \mathcal{R}^2$, which are unisolvent for π_1^2. The construction is appealing in that for "interior" points x_j of X it is local. That is, for such points the entries in the j-th column of Q depend only on the geometry of the nodes near x_j and not on any properties of nodes far away.

Choose W as a closed bounded convex polygonal region of $\mathcal{R}^2$ such that $X \subset W$. Suppose without loss of generality that $\{x_{N-2}, x_{N-1}, x_N\}$ is unisolvent for π_1^2. We will refer to these points as special points. They are generally chosen so that they are well spread throughout W. In our experience, and that of Sibson and Stone, for typical data sets the choice of special points is not at all critical, as long as the triangle they define

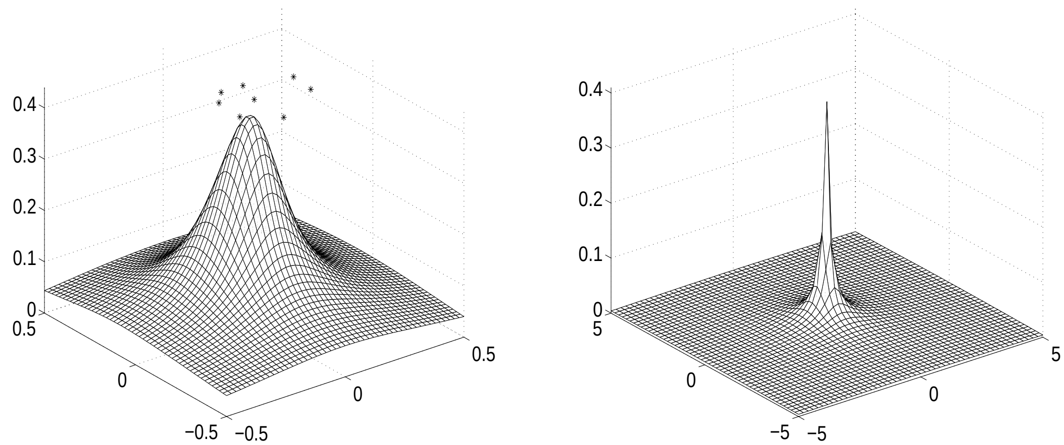

(a) (b)

Figure 2: Ψ elements for the preconditioner of this paper. Multiquadric basic function.

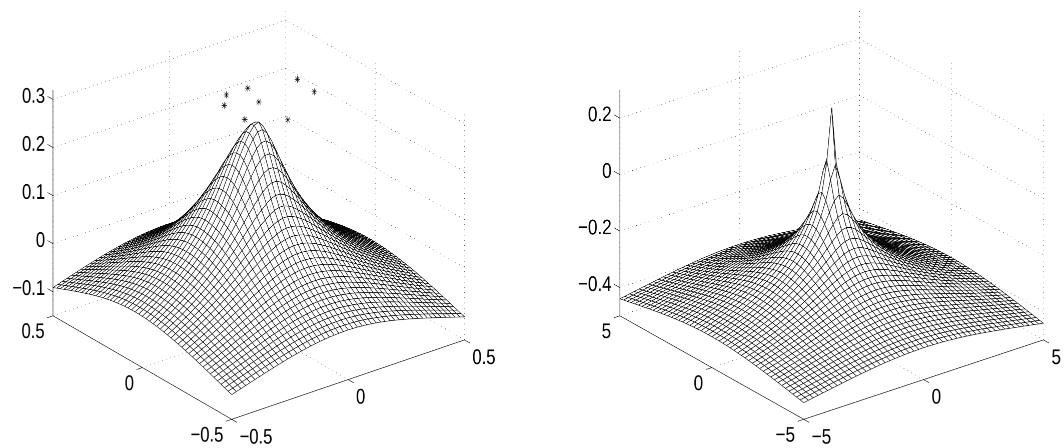

(a) (b)

Figure 3: Ψ elements for the preconditioner of this paper. Thin-plate spline basic function.

has largish area. However, for contrived data sets, such as all but a very few points on a straight line, the choice of special points becomes important. In these cases we have observed that bad choices of special points can lead to large condition numbers. However, the strategy of choosing the three special points to maximise the area of the corresponding triangle has always led to small condition numbers.

The region W is first divided into panels by intersecting a Voronoi diagram of the points of X with the region W. We denote this panelling of W by

$$V_W(X) = \bigcup_{i=1}^{N} V_i$$

where V_i is the Voronoi panel about the ith centre and is defined by

$$V_i = \{x \in W : |x - x_i| < |x - x_j|, \quad \text{for all } 1 \leq j \leq N \text{ with } j \neq i\}.$$

Recall that the locus of points equidistant from two fixed points is the perpendicular bisector of the segment connecting the points. It follows that each Voronoi region is polygonal. Associated with a panel V_i are its edges. These are a finite number of distinct closed line segments of non-zero length. They are the boundaries between different Voronoi panels, or between a Voronoi panel and W^C. The collection of all edges of all the Voronoi panels will be denoted by $\mathcal{E}$.

Definition 2.1. *Two polygonal regions of $\mathcal{R}^2$ will be said to be strongly contiguous if they have a common boundary of non-zero length.*

Definition 2.2. *Two Voronoi regions V_i and V_j will be said to be C-related if there is a sequence*

$$\{V_i, V_{\ell_1}, V_{\ell_2}, \dots, V_{\ell_m}, V_j\}, \qquad 1 \leq i, j, \ell_1, \dots, \ell_m \leq N - 3,$$

in which all adjacent pairs are strongly contiguous.

Loosely speaking V_i and V_j are C-related if they are connected by a chain of strongly contiguous pairs. C-related is an equivalence relation on the set $\{V_i\}_{i=1}^{N-3}$ of Voronoi regions of non-special points. Therefore it breaks this set into a finite number of nonempty equivalence classes $\{\mathcal{G}_l : 1 \leq l \leq k\}$. Figure 4 illustrates the different equivalence classes of strongly contiguous sets of Voronoi panels arising from different choices of the three special points.

Lemma 2.3. *Let $\mathcal{G}_\ell$ be any of the equivalence classes above. Then there is at least one Voronoi region V_i in $\mathcal{G}_\ell$ which is strongly contiguous to either W^C or one of $\{V_{N-2}, V_{N-1}, V_N\}$.*

Proof. Consider

$$T = \bigcup_{i : V_i \in \mathcal{G}_\ell} \overline{V_i}$$

This union is a closed bounded connected polygonal set whose boundary can be written as the union of some of the line segments from $\mathcal{E}$. Recall in particular that all these line segments have non-zero length. Pick one line segment $< a, b >$ from the boundary of T. Since it forms part of the boundary of T on one side of it lies a Voronoi region V_i from $\mathcal{G}_\ell$. On the other side lies either W^C or another Voronoi region V_j. In the first case the Lemma is proven. Consider the second case. If $1 \leq j \leq N - 3$ then V_i is strongly contiguous to V_j. Consequently, $V_j \in \mathcal{G}_\ell$. This contradicts $< a, b >$ being on the boundary of T. Hence, $N - 2 \leq j \leq N$ and the Lemma follows. □

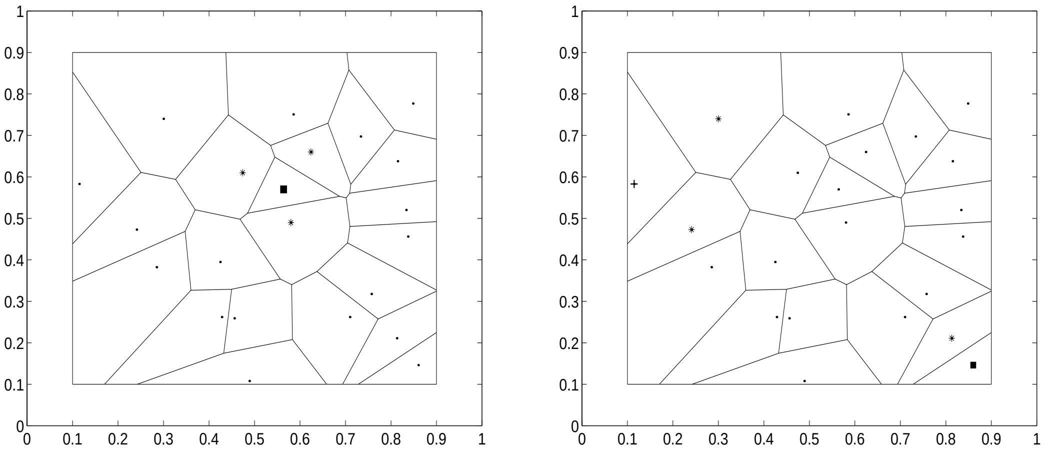

(a) A configuration of special points ($*$) leading to two strongly contiguous sets of Voronoi panels.

(b) A configuration of special points ($*$) leading to three strongly contiguous sets of Voronoi panels.

Figure 4: Configurations of points where E (see equation (9)) is reducible. In each figure centres in the same strongly contiguous regions share the same symbol, and $*$'s denote special points.

We now detail the construction of the $N \times (N-3)$ matrix Q using boundary over distance weights. Note that because most elements of Q are zero sparse storage of Q requires only $\mathcal{O}(N)$ memory. A non-special point from $\{x_i : 1 \leq i \leq N-3\}$ which is strongly contiguous to W^C will be called a *Voronoi external point*. Define $V_E(X)$ as the set of indices of all Voronoi external points. All other points are referred to as *Voronoi internal points*. The corresponding indices are $V_I(X) = \{1, \ldots, N-3\} - V_E(X)$. See Figure 5 for examples of Voronoi internal and external points.

We first consider forming a column of Q for an index, j, such that $j \in V_I(X)$. In this case the panel V_j shares non-trivial edges only with other Voronoi panels and not with W^C. The column is formed using boundary over distance weights, found from the Voronoi diagram. For $j \in V_I(X)$ the boundary over distance weight r_{ij} is

$$r_{ij} = \frac{b(x_i, x_j)}{|x_i - x_j|}, \qquad \text{for all } V_i \text{ strongly contiguous to } V_j, \tag{6}$$

where $b(x_i, x_j)$ is the length of the boundary between V_i and V_j. For other values of $i \neq j$, r_{ij} is set to zero. In order that column j of Q is orthogonal to constants the diagonal element r_{jj} is specified as

$$r_{jj} = -\sum_{i \neq j} r_{ij}.$$

Finally, the jth column of R is scaled by dividing by the area of V_j to obtain the jth column

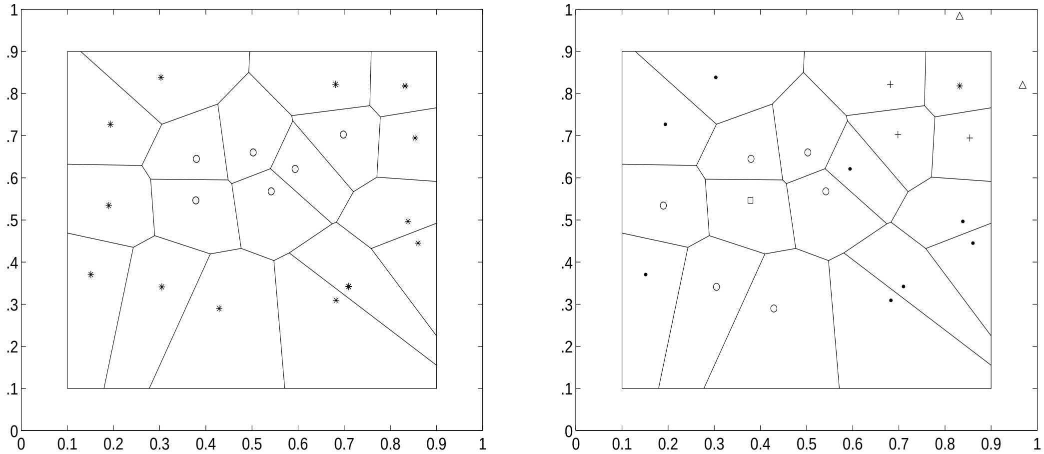

(a) Internal centres (o) and external centres ($*$) of X.

(b) The neighbours (o) of an internal centre (□) and neighbours (+) of an external centre ($*$). Artificial points corresponding to the external centre $*$ are denoted by △.

Figure 5: Voronoi panelling of a set of twenty data points in the region $W = [.1, .9]^2$.

of Q. Note that the column is by construction diagonally dominant, but not strictly so.

If $j \in V_E(X)$ then V_j is strongly contiguous to the complement of W, W^C. The boundary segment corresponds to a Voronoi edge between x_j and an artificial point, the reflection of x_j in the boundary (see Figure 5(b)). The reflected point, $\hat{x}_j$, can be written as a linear combination of the special points, i.e.,

$$\hat{x}_j = \lambda_N x_N + \lambda_{N-1} x_{N-1} + \lambda_{N-2} x_{N-2}, \tag{7}$$

where $\lambda_N + \lambda_{N-1} + \lambda_{N-2} = 1$. If V_j has k edges with W^C then k reflected points $\{\hat{x}_j^1, \ldots, \hat{x}_j^k\}$ are required. Associated with each reflected point, $\hat{x}_j^a$, are the coefficients $\{\lambda_N^a, \lambda_{N-1}^a, \lambda_{N-2}^a\}$. The boundary over distance weights for $\hat{x}_j^a$ are partitioned amongst the special points to obtain for all $j \in V_E(X)$ and $i \neq j$

$$r_{ij} = \begin{cases} \frac{b(x_i,x_j)}{|x_i - x_j|}, & V_i \text{ strongly contiguous to } V_j, \\ \sum_{l=1}^{k} \lambda_i^l \frac{b(\hat{x}_j^l, x_j)}{|\hat{x}_j^l - x_j|}, & i \in \{N, N-1, N-2\}. \end{cases} \tag{8}$$

Of course, V_j could be strongly contiguous with a Voronoi panel associated with a special point. If this is the case $r_{ij} = \frac{b(x_i,x_j)}{|x_i - x_j|} + \sum_{l=1}^{k} \lambda_i^l \frac{b(\hat{x}_j^l, x_j)}{|\hat{x}_j^l - x_j|}$. Again, for other values of $i \neq j$, r_{ij} is set to zero and column j of Q is column j of R scaled by dividing by the area of V_j.

Partition Q as

$$Q = \begin{bmatrix} E \\ F \end{bmatrix}, \tag{9}$$

where E is $(N-3)\times(N-3)$. Thus E results from interactions between non-special points, and F those between special and non-special points. Note in the construction above that for $1 \le i, j \le N-3$, e_{ij} is non-zero if and only if V_i is strongly contiguous to V_j. Furthermore, note that E is necessarily column diagonally dominant, with strict dominance in column j whenever V_j is strongly contiguous to the Voronoi region of a special point, or to W^C.

Relabelling if necessary we can assume the indices of the Voronoi regions in each of the equivalence classes $\mathcal{G}_i$ form a contiguous subset of $\{1, \ldots, N-3\}$. Similarly, we can also assume that the indices corresponding to any $\mathcal{G}_i$ precede those corresponding to $\mathcal{G}_{i+1}$. Furthermore, by construction if $i \neq j$ none of the regions in $\mathcal{G}_i$ is strongly contiguous with a region in $\mathcal{G}_j$. Thus, corresponding entries in the matrix E constructed using boundary over distance weights and artificial points are zero. That is E is block diagonal with the square matrix E_{ii} on the main diagonal corresponding to the equivalence class of Voronoi regions $\mathcal{G}_i$. More precisely, Q will have form

$$Q = \begin{bmatrix} E_{11} & O & \cdots & O \\ O & E_{22} & \cdots & O \\ \vdots & \vdots & \ddots & \vdots \\ O & O & \cdots & E_{kk} \\ F_1 & F_2 & \cdots & F_k \end{bmatrix}. \tag{10}$$

3 Properties of the matrix Q

In this section we establish the fundamental properties of the matrix Q of (10). Namely that it is of full rank and that its columns are orthogonal to those of P.

Definition 3.1. *For $m \ge 2$, an $m \times m$ matrix K is* irreducible *if there does not exist an $m \times m$ permutation matrix P such that*

$$PKP^T = \begin{bmatrix} M_{11} & M_{12} \\ 0 & M_{22} \end{bmatrix},$$

where M_{11} is $r \times r$, M_{22} is $(m-r)\times(m-r)$, and $1 \le r < m$.

The following result is well known, see for example Varga [14].

Theorem 3.2. *Suppose the square matrix K is irreducible and row (column) diagonally dominant with strict row (column) diagonal dominance in at least one row (column). Then K is invertible.*

The proof of the following result relies on the concept of directed graphs from graph theory. The directed graph, $G(K)$, of a matrix K, is a graph such that there is a directed arc between vertices y_i and y_j of the graph if and only if the entry k_{ij} of the matrix is non-zero.

Definition 3.3. *A directed graph is* strongly connected *if for any pair of points y_i and y_j there exists a directed path $\overrightarrow{y_i y_{l_1}}, \overrightarrow{y_{l_1} y_{l_2}}, \dots, \overrightarrow{y_{l_{k-1}} y_j}$, connecting y_i to y_j.*

Lemma 3.4. *(Theorem 1.6 of Varga [14]) A square complex matrix K is irreducible if and only if its directed graph $G(K)$ is strongly connected.*

Lemma 3.5. *Let X be a finite set of distinct points unisolvent for π_1^2. Let E_{ii} be one of the square blocks from the diagonal of Q constructed in the previous section. Then E_{ii} is invertible.*

Proof. ¿From the construction E_{ii} is column diagonally dominant. Furthermore, by Lemma 2.3 the diagonal dominance is strict for at least one column of E_{ii}. ¿From the definition of the equivalence relation C-related there is a chain of strongly contiguous pairs of Voronoi regions, connecting any two Voronoi regions in $\mathcal{G}_i$. This implies the corresponding entries in E_{ii} are non-zero and hence from Lemma 3.4 E_{ii} is irreducible. It follows from Theorem 3.2 that E_{ii} is invertible. □

Theorem 3.6. *The matrix Q described in Section 2 is orthogonal to P.*

Proof. It suffices to show that the matrix R (which is Q before column scaling) is orthogonal to P. The proof of this theorem for interior nodes is taken from Christ et.al. [6, Theorem 1]. Let $j \in V_I(X)$. If we let v be a constant vector then from the divergence theorem

$$0 = \int_{V_j} \nabla \cdot v \, dt = \int v \cdot n \, dS,$$

where n is a normal vector and S is the boundary of V_j.

Each boundary segment of V_j is associated with a contiguous Voronoi panel. Let $\mathcal{S}_j$ be the set of indices of such contiguous panels. For $i \in \mathcal{S}_j$ the length of the boundary between V_j and V_i is given by $b(x_j, x_i)$. From the properties of a Voronoi diagram an outward normal to this boundary is $\frac{x_i - x_j}{|x_i - x_j|}$. Integrating over each of these boundaries separately gives

$$0 = \int v \cdot n \, dS = v \cdot \sum_{i \in \mathcal{S}_j} \frac{b(x_i, x_j)}{|x_i - x_j|}(x_i - x_j). \tag{11}$$

Because v is any constant vector we obtain

$$\sum_{i \in \mathcal{S}_i} \frac{b(x_i, x_j)}{|x_i - x_j|}(x_i - x_j) = 0, \tag{12}$$

and the result follows from $r_{jj} = -\sum_{i\in\mathcal{S}_j} r_{ij}$. Note the interesting alternative interpretation of (12) as an expression for x_j as a convex combination of its neighbours.

For $j \in V_E(X)$ we have at least one boundary segment of V_j which corresponds to a boundary between V_j and W^C. In the case of only one boundary segment between V_j and W^C we introduce the corresponding artificial point $\hat{x}_j = \lambda_n x_n + \lambda_{n-1}x_{n-1} + \lambda_{n-2}x_{n-2}$. Then

$$\begin{aligned} v \cdot \sum_{i\neq j} r_{ij}(x_j - x_i) \\ &= v \cdot \left(\sum_{i\in\mathcal{S}_j} r_{ij}(x_j - x_i) + r_{n,j}(x_j - x_n) + r_{n-1,j}(x_j - x_{n-1}) + r_{n-2,j}(x_j - x_{n-2}) \right), \\ &= v \cdot \left(\sum_{i\in\mathcal{S}_j} r_{ij}(x_j - x_i) + \frac{b(\hat{x}_j, x_j)}{|\hat{x}_j - x_j|}(x_j - \hat{x}_j) \right), \\ &= \int v \cdot n \, dS = 0, \end{aligned} \tag{13}$$

where the last line follows from (11) and because $\frac{x_j - \hat{x}_j}{|\hat{x}_j - x_j|}$ is a normal vector to the boundary between V_j and W^C. The result again follows from $r_{jj} = -\sum_{i\neq j} r_{ij}$. If V_j has more then one boundary with W^C then the proof can be easily extended by using more artificial points in (13). □

Theorem 3.7. *Let X be a set of distinct points unisolvent for π_1^2. Let Q be formed by the construction in Section 2 and $A_{ij} = \Phi(x_i - x_j)$ where Φ is strictly conditionally positive definite of order 2. Then $B = Q^T AQ$ is positive definite.*

Proof. ¿From Lemma 3.5 each of the matrices E_{ii} occurring in the block partitioning of Q given in Equation (10) is invertible. Hence Q has full rank. Also from Theorem 3.6 the columns of Q are orthogonal to the columns of P. Let μ be any non-zero vector in $\mathcal{R}^{N-3}$, and define $\lambda = Q\mu$. Then $\lambda \neq 0$, $P^T\lambda = P^TQ\mu = 0$, and $\mu^T B\mu = \mu^T Q^T AQ\mu = \lambda^T A\lambda$. Hence, by the definition of strictly conditionally positive definite, $\mu^T B\mu > 0$ whenever $\mu \neq 0$ and B is symmetric positive definite. □

4 Scaleability

In this section we show that for certain functions Φ the new interpolation matrix $B = Q^T AQ$ is a homogeneous function of scale. Thus its condition number, and the relative spread of its eigenvalues, are scale independent. If the interpolation matrix is not a homogeneous function of scale then the condition number can change dramatically over different scales. This is important for fitting methods such as those described in [2] and [1], where solutions to systems on many different scales are required.

Lemma 4.1. *Given $X = \{x_1, \ldots, x_N\}$ unisolvent with respect to π^d_{k-1}. Let $\{r_1, \ldots, r_N\}$ and $\{s_1, \ldots, s_N\}$ satisfy $\sum_{j=1}^N r_j q(x_j) = 0$, and $\sum_{j=1}^N s_j q(x_j) = 0$, for all $q \in \pi^d_{k-1}$. Define $T : C(\mathcal{R}^d \times \mathcal{R}^d) \to \mathcal{R}$ by*

$$Tg = \sum_{i,j=1}^N r_i s_j g(x_i, x_j), \tag{14}$$

for $g \in C(\mathcal{R}^d \times \mathcal{R}^d)$. Then T annihilates all functions g of the form $g(x, y) = p(x - y)$ with $p \in \pi^d_{2k-1}$.

Proof. Following [1, Lemma 2.1] we let $p(x) = p_\alpha(x) = x^\alpha$, where $x \in \mathcal{R}^d$ and $\alpha \in Z^d_+$ with $|\alpha| < 2k$. From the binomial theorem we have

$$g(x, y) = p(x - y) = \sum_{0\le\beta\le\alpha} a_\beta x^{\alpha-\beta} y^\beta = \sum_{0\le\beta\le\alpha} a_\beta p_{\alpha-\beta}(x) p_\beta(y),\ x, y \in \mathcal{R}^d,$$

Define $g_{\alpha\beta} = p_{\alpha-\beta}(x)p_\beta(y)$, then

$$Tp_\alpha = \sum_{0\le\beta\le\alpha} a_\beta T g_{\alpha\beta}.$$

Now, from (14)

$$\begin{aligned} Tg_{\alpha\beta} &= \sum_{i,j=1}^N r_i s_j g_{\alpha\beta}(x_i, x_j), \\ &= \sum_{i,j} r_i s_j p_{\alpha-\beta}(x_i) p_\beta(x_j), \\ &= \left(\sum_i r_i p_{\alpha-\beta}(x_i) \right) \left(\sum_j s_j p_\beta(x_j) \right). \end{aligned} \tag{15}$$

¿From the hypothesis, and because either $|\beta| \le k - 1$ or $|\alpha - \beta| \le k - 1$, one of the bracketed expressions is zero. Hence Tg is zero. □

Theorem 4.2. *Let the symmetric function $\Phi \in C(\mathcal{R}^d \times \mathcal{R}^d)$ be such that $\Phi(hx, hy) = h^\gamma \Phi(x, y) + p_h(x - y)$ for all $h > 0$ and $x, y \in \mathcal{R}^d$, where $\gamma \in \mathcal{R}$ and $p_h \in \pi^d_{2k-1}$. Let $X = \{x_1, \ldots, x_N\}$ be a unisolvent set of points with respect to π^d_{k-1} and let $\{r_1, \ldots, r_N\}$ and $\{s_1, \ldots, s_N\}$ be as in Lemma 4.1. Define the functional $T_h\Phi$ by*

$$T_h\Phi = \sum_{i,j=1}^N r_i s_j \Phi(hx_i, hx_j),$$

and write T for T_1. Then for $h > 0$, $T_h\Phi = h^\gamma T\Phi$.

Proof. ¿From the definition we have

$$\begin{aligned} T_h\Phi &= \sum_{i,j} r_i s_j \Phi(hx_i, hx_j), \\ &= \sum_{i,j} r_i s_j \left\{h^\gamma \Phi(x_i, x_j) + p_h(x_i - x_j)\right\}, \\ &= h^\gamma T\Phi + Tv, \end{aligned} \tag{16}$$

where $v(x, y) = p_h(x - y)$ for some $p_h \in \pi^d_{2k-1}$ and T is as in Lemma 4.1. From that lemma $Tv = 0$ and the Theorem follows. □

In the following Theorem matrices with a subscript h are defined in the same way as the matrix without the subscript except with the point set hX instead of X.

Theorem 4.3. *Let $X = \{x_1, \dots, x_N\}$ be unisolvent with respect to π^d_{k-1}, and P be defined by $P_{ij} = p_j(x_i)$, where $p_1, \dots, p_l$ is a basis for π^d_{k-1}. Let Q_h be any $N \times (N - dim(\pi^d_{k-1}))$ matrix which depends homogeneously on the scale parameter h such that $Q_h = h^\nu Q$, and $P^T Q = 0$.*

Then if $\Phi(hx, hy) = h^\gamma \Phi(x, y) + p_h(x - y)$, $h > 0$ for some $p_h \in \pi^d_{2k-1}$, B_h is a homogeneous function of h. Specifically

$$B_h = h^{2\nu+\gamma} B.$$

Proof. Let r_j be the jth column of Q. Then from Theorem 4.2 and the condition on Φ we have,

$$r_j^T A_h r_i = h^\gamma r_j^T A r_i,$$

and so

$$Q^T A_h Q = h^\gamma Q^T A Q = h^\gamma B. \tag{17}$$

¿From the conditions on Q and (17)

$$\begin{aligned} B_h &= Q_h^T A_h Q_h, \\ &= h^{2\nu} Q^T A_h Q, \\ &= h^{2\nu+\gamma} B. \end{aligned}$$

□

Remark 4.4. *If Φ is the basic function $\Phi(\cdot) = (-1)^k |\cdot|^{2(k-1)} \log|\cdot|$ then from the proof of Corollary 2.3 in [1] we have,*

$$\Phi(hx, hy) = h^{2(k-1)} \Phi(x, y) + p_h(x - y), \tag{18}$$

where $p_h \in \pi^d_{2(k-1)}$. So the thin-plate spline basic function satisfies the condition on Φ in Theorem 4.3.

Corollary 4.5. *Let Φ be strictly conditionally positive definite of order 2 and such that $\Phi(hx, hy) = h^\gamma \Phi(x, y) + p_h(x - y), h > 0$ with $p_h \in \pi_3^2$. Then the interpolation matrix, B_h, produced by the algorithm in Section 2 is a homogeneous function of scale.*

Proof. ¿From Theorem 4.3 it is sufficient to show that $Q_h = h^\nu Q$, for some ν. The Voronoi diagram scales homogeneously hence $b(hx_i, hx_j) = hb(x_i, x_j)$. Also, the area of the panel associated with hx_i is h^2 times that of the panel associated with x_i. Therefore, we have for $Q_{ij} \neq 0$, $j \in V_I(X)$, $i \neq j$,

$$(Q_h)_{ij} = \frac{b(hx_i, hx_j)}{|h(x_i - x_j)|h^2 A(V_i)} = h^{-2} Q_{ij}.$$

Noticing that $\{\lambda_n, \lambda_{n-1}, \lambda_{n-2}\}$ in (7) are unchanged by scale gives $(Q_h)_{ij} = h^{-2} Q_{ij}$, $j \in V_E(X)$. □

Theorem 4.6. *Let Φ be strictly conditionally positive definite of order 2 and such that $\Phi(hx, hy) = h^\gamma \Phi(x, y) + p_h(x - y), h > 0$ with $p_h \in \pi_3^2$. Then the interpolation matrix, S, produced by scaling the matrix B so that $S = DBD$, where D is diagonal and $D_{ii} = 1/\sqrt{B_{ii}}$, is constant over all scales.*

Proof. ¿From Corollary 4.5, $B_h = h^\theta B$, for some θ. So $d_{ii}^h = (b_{ii}^h)^{-\frac{1}{2}} = h^{-\frac{\theta}{2}} d_{ii}$ and $S_h = D_h B_h D_h = h^{-\theta} D B_h D = h^{-\theta} h^\theta DBD = S$. □

5 Decay

The dramatic improvement in conditioning between the unpreconditioned matrix and the preconditioned matrix is due to the localisation of the preconditioner. Specifically, in this section we show that these local preconditioners have the property that $|B_{ij}| \approx \|x_i - x_j\|^{-\kappa}$ as $\|x_i - x_j\|$ grows, where κ is three for the multiquadric and two for the thin-plate spline. This decay means the interpolation matrix is "almost" diagonally dominant and thus better conditioned. In this section $|\cdot|$ applied to a multiindex means its 1-norm.

Definition 5.1. *Given the points $X = \{x_1, \ldots, x_{N+1}\} \subset \mathcal{R}^2$. The set $\mathcal{U}_X \subset \mathcal{R}^{N+1}$ consists of all $\beta \in \mathcal{R}^{N+1} \backslash \{0\}$ that satisfy*

$$\sum_{i=1}^{N+1} \beta_i q(x_i) = 0, \text{ for all } q \in \pi_1^2. \tag{19}$$

In this section we denote the set $\mathcal{S}_j$ to be all the indices i such that V_i is strongly contiguous with V_j. Note that $j \notin \mathcal{S}_j$.

Lemma 5.2. *Let x_j be an internal node of a Voronoi diagram. The area of a Voronoi polygon, V_j, about x_j, is given by*

$$\frac{1}{4} \sum_{i \in \mathcal{S}_j} \|x_j - x_i\| b(x_j, x_i),$$

where $b(x_j, x_i)$ is the length of the Voronoi boundary orthogonal to $x_j - x_i$.

Proof. A Voronoi polygon of x_j can be divided into triangles by line segments between x_j and the vertices of the polygon. The area of each of these triangles can easily be shown to be $\|x_j - x_i\| b(x_j, x_i)/4$. Summing these areas gives the result. □

Lemma 5.3. *Let x_j be an internal node and V_j the corresponding Voronoi panel. Then if $\beta_i = \frac{b(x_j,x_i)}{\|x_j-x_i\|}$, $i \in \mathcal{S}_j$,*

$$\left| \sum_{i\in\mathcal{S}_j} \beta_i (x_j - x_i)^\alpha \right| \le 4 Area(V), \text{ for } |\alpha| = 2. \tag{20}$$

Proof. Noticing that $|(x_j - x_i)^\alpha| \le \|x_j - x_i\|^2$ for $|\alpha| = 2$ we have

$$\begin{aligned} \left| \sum_{i\in\mathcal{S}_j} \beta_i (x_j - x_i)^\alpha \right| &\le \sum_{i\in\mathcal{S}_j} \beta_i |(x_j - x_i)^\alpha|, \\ &\le \sum_{i\in\mathcal{S}_j} \beta_i \|x_j - x_i\|^2, \\ &= \sum_{i\in\mathcal{S}_j} \frac{b(x_j, x_i)}{\|x_j - x_i\|} \|x_j - x_i\|^2, \\ &= 4\text{Area}(V), \end{aligned}$$

by Lemma 5.2. □

Lemma 5.4. *Let $f(\cdot) := |\cdot|^{-k}$, $k > 0$ so that $f : \mathcal{R}^2 \backslash \{0\} \to \mathcal{R}$. Then if $\mathcal{D}^\alpha$, $\alpha \in \mathcal{N}^2$, is the differential operator*

$$\frac{\partial^{\alpha_1+\alpha_2}}{\partial \xi^{\alpha_1} \partial \eta^{\alpha_2}},$$

where $x = (\xi, \eta)$ we have

$$\mathcal{D}^\alpha f(\cdot) = \frac{P_\alpha(\cdot)}{|\cdot|^{k+2|\alpha|}}, \tag{21}$$

where P_α is a homogeneous polynomial of degree $|\alpha|$.

Proof. Let $|\alpha| = 1$, then

$$\begin{aligned} \mathcal{D}^\alpha f(x) &= \mathcal{D}^\alpha (|x|^{-k}), \\ &= \frac{-k x^\alpha}{|x|^{k+2}}, \end{aligned}$$

as required. Now assume that (21) holds for $|\alpha| = n$. If $|\gamma| = 1$ we obtain

$$\begin{aligned}
\mathcal{D}^{\alpha+\gamma} f(x) &= \mathcal{D}^{\gamma}\left(\frac{P_\alpha(x)}{|x|^{k+2n}}\right), \\
&= \frac{\mathcal{D}^{\gamma}(P_\alpha(x))|x|^{k+2n} - \mathcal{D}^{\gamma}(|x|^{k+2n})P_\alpha(x)}{|x|^{2(k+2n)}}, \\
&= \frac{\hat{P}_{\alpha-1}(x)|x|^2 - (k+2n)P_\alpha(x)x^\gamma}{|x|^{k+2(n+1)}}. \qquad (22)
\end{aligned}$$

In (22) $\hat{P}_{\alpha-1} = \mathcal{D}^{\gamma}(P_\alpha(x))$ is a homogeneous polynomial of degree $n-1$. The result follows from setting $P_{\alpha+\gamma}(x) = \hat{P}_{\alpha-1}(x)|x|^2 - (k+2n)P_\alpha(x)x^\gamma$. □

Lemma 5.5. *Let $X = \{x_1, \dots, x_{N+1}\}$, $x_i = (\xi_i, \eta_i) \in \mathcal{R}^2\backslash\{0\}$, be $N+1$ distinct points contained in the circle $|\cdot - x| \le H < |x|$ where $x = x_{N+1}$. If $\beta \in \mathcal{U}_X$, and $n, \alpha > 0$ then,*

$$\left|\sum_{i=1}^{N+1} \beta_i \frac{x_i^\alpha}{|x_i|^n}\right| \le \frac{H^2 DE}{|x|^{n-|\alpha|+2}} + \mathcal{O}(|x|^{-(n-|\alpha|+3)}),$$

where $E = \sum_{i=1}^{N} |\beta_i|$ and D depends on α and n. Furthermore, if $\beta_i = \frac{b(x_i,x)}{\|x_i - x\|}$, $i = 1, \dots, N$ then

$$E = \frac{4Area(V)}{H^2},$$

where V is the Voronoi region about the point x.

Proof. Let $h_i = (\Delta\xi_i, \Delta\eta_i) = x - x_i$. Now we obtain via the binomial expansion

$$\begin{aligned}
(x - h_i)^\alpha &= \sum_{k=0}^{\alpha_1}\sum_{j=0}^{\alpha_2} \binom{\alpha_1}{k}\binom{\alpha_2}{j} \xi^k \eta^j (-\Delta\xi_k)^{\alpha_1-k}(-\Delta\eta_k)^{\alpha_2-j}, \\
&= \sum_{l=0}^{|\alpha|} \sum_{k=\max\{0,l-\alpha_2\}}^{\min\{l,\alpha_1\}} \binom{\alpha_1}{k}\binom{\alpha_2}{l-k} (-1)^{|\alpha|-l} \xi^k \eta^{l-k} \Delta\xi_k^{\alpha_1-k} \Delta\eta_k^{\alpha_2+k-l}, \\
&= \sum_{l=0}^{|\alpha|} P_l(x, h_i, \alpha), \qquad (23)
\end{aligned}$$

where $P_l(x, h_i, \alpha)$ is a polynomial of degree l in x and $|\alpha| - l$ in h_i.

By a Taylor's expansion in h about x and using Lemma 5.4, or alternatively using that $(1 - 2xy + y^2)^{-n}$ is the generating function for a family of Gegenbauer polynomials [13, 4.7.23], we have

$$|x_i|^{-n} = |x - h_i|^{-n} = |x|^{-n} \sum_{m=0}^{\infty} \frac{Q_m(x, h_i, n)}{|x|^{2m}}, \quad |h_i| < |x|, \qquad (24)$$

where in (24) $Q_m(x,h,n)$ is a polynomial of degree m in x and h.

Now using (19) and combining (23) and (24)

$$\sum_{i=1}^{N+1} \beta_i \frac{x_i^\alpha}{|x_i|^n} = \sum_{i=1}^{N} \beta_i \left(\frac{(x-h_i)^\alpha}{|x_i|^n} - \frac{x^\alpha}{|x|^n} \right),$$
$$= \frac{1}{|x|^n} \sum_{i=1}^{N} \beta_i \left(\sum_{l=0}^{|\alpha|} P_l(x,h_i,\alpha) \sum_{m=0}^{\infty} \frac{Q_m(x,h_i,n)}{|x|^{2m}} \right) - \frac{1}{|x|^n} \sum_{i=1}^{N} \beta_i x^\alpha. \tag{25}$$

In the series on the left all terms that arise are of order $-n+|\alpha|-\gamma$ in x, $\gamma \geq 0$. Those of order $-n+|\alpha|-\gamma$ correspond to values of l and m such that $m-l=\gamma-|\alpha|$. The restrictions on m and l are as in (25). The lemma will be proved by showing that the terms corresponding to $\gamma=0,1$ vanish.

Firstly consider $\gamma=0$; then $m=0$ and $l=|\alpha|$ and the corresponding terms in (25) of order $-n+|\alpha|$ are

$$\frac{1}{|x|^{n+1}} \sum_{i=1}^{N} \beta_i \Big(P_{|\alpha|}(x,h_i,\alpha) Q_0(x,h_i,n) - x^\alpha \Big) = 0,$$

because $P_{|\alpha|}(x,h,\alpha)=x^\alpha$ and $Q_0(x,h,n)=1$. For $\gamma=1$; $(l,m)=(|\alpha|,1)$ and $(|\alpha|-1,0)$. Expanding the functions P and Q for these values of (l,m) gives the terms

$$-\frac{1}{|x|^{n+1}} \sum_{i=1}^{N} \beta_i \left(\binom{\alpha_1}{\alpha_1-1} \xi^{\alpha_1-1}\eta^{\alpha_2}\Delta\xi_i + \binom{\alpha_2}{\alpha_2-1} \xi^{\alpha_1}\eta^{\alpha_2-1}\Delta\eta_i \right) = 0, \tag{26}$$

from (19). This leaves us with the most positive power of $|x|$ being $-(n-|\alpha|+2)$ as required. These terms correspond to values of $(l,m)=(|\alpha|-2,0);(|\alpha|-1,1)$; and $(|\alpha|,2)$. The terms in (25) of exact order $|x|^{-(n-|\alpha|+2)}$ are

$$\frac{1}{|x|^4}\Big(|x|^4 Q_0 P_{|\alpha|-2} + |x|^2 Q_1 P_{|\alpha|-1} + Q_2 P_{|\alpha|-2}\Big)$$
$$= \frac{x^\alpha}{|x|^4}\Big(\xi^2(\Delta\xi_i^2 c_1 + \Delta\eta_i^2 c_4) + \eta^2(\Delta\xi_i^2 c_5 + \Delta\eta_i^2 c_2)$$
$$+ \xi\eta\Delta\xi_i\Delta\eta_i c_3 + \xi^{-1}\eta^3\Delta\xi_i\Delta\eta_i c_6 + \xi^3\eta^{-1}\Delta\xi_i\Delta\eta_i c_7$$
$$+ \xi^{-2}\eta^4\Delta\xi_i^2 c_8 + \xi^4\eta^{-2}\Delta\eta_i^2 c_9\Big), \tag{27}$$

where

$$\begin{aligned}
c_1 &= -n\alpha_1 + \frac{1}{2}\alpha_1(\alpha_1 - 1),\\
c_2 &= -n\alpha_2 + \frac{1}{2}\alpha_2(\alpha_2 - 1),\\
c_3 &= n(1 - |\alpha|) + 2\alpha_1\alpha_2,\\
c_4 &= -n(\frac{1}{2} + \alpha_2) + \alpha_2(\alpha_2 - 1),\\
c_5 &= -n(\frac{1}{2} + \alpha_1) + \alpha_1(\alpha_1 - 1),\\
c_6 &= \alpha_1(\alpha_2 - n),\\
c_7 &= \alpha_2(\alpha_1 - n),\\
c_8 &= \frac{1}{2}\alpha_1(\alpha_1 - 1),\\
c_9 &= \frac{1}{2}\alpha_2(\alpha_2 - 1).
\end{aligned}$$

By taking absolute values and noticing that $|x^\alpha| \le |x|^{|\alpha|}$ we obtain from (27)

$$\begin{aligned}
\frac{1}{|x|^4}&\Big(|x|^4 Q_0 P_{|\alpha|-2} + |x|^2 Q_1 P_{|\alpha|-1} + Q_2 P_{|\alpha|-2}\Big)\\
&\le \frac{|x|^{|\alpha|+2}}{|x|^4}\Big(\Delta\xi_i^2 d_1 + |\Delta\xi_i\Delta\eta_i| d_2 + \Delta\eta_i^2 d_3\Big),\\
&= \frac{1}{|x|^{-|\alpha|+2}}\Big(\Delta\xi_i^2 d_1 + |\Delta\xi_i\Delta\eta_i| d_2 + \Delta\eta_i^2 d_3\Big),
\end{aligned} \tag{28}$$

where $d_1 = |c_1|+|c_5|+|c_8|$, $d_2 = |c_3|+|c_6|+|c_7|$, and $d_3 = |c_2|+|c_4|+|c_9|$. Now substituting (28) into equation (25) we obtain

$$\begin{aligned}
\left|\sum_{i=1}^{N+1}\beta_i\frac{x_i^\alpha}{|x_i|^n}\right| &\le \frac{1}{|x|^{n-|\alpha|+2}}\sum_{i=1}^{N}|\beta_i|\Big(\Delta\xi_i^2 d_1 + |\Delta\xi_i\Delta\eta_i| d_2 + \Delta\eta_i^2 d_3\Big) + \left|\mathcal{O}(|x|^{-(n-|\alpha|+3)})\right|,\\
&\le \frac{H^2 DE}{|x|^{n-|\alpha|+2}} + \left|\mathcal{O}(|x|^{-(n-|\alpha|+3)})\right|,
\end{aligned} \tag{29}$$

where $E = \sum_{i=1}^{N}|\beta_i|$ and $D = d_1 + d_2 + d_3$. If we take β_i to be boundary over distance weights then using Lemma 5.3 gives the bound

$$\left|\sum_{i=1}^{N+1}\beta_i\frac{x_i^\alpha}{|x_i|^n}\right| \le \frac{4\text{Area}(V)D}{|x|^{n-|\alpha|+2}} + \left|\mathcal{O}(|x|^{-(n-|\alpha|+3)})\right|.$$

□

The following two theorems show that for local preconditioners the entries of the preconditioned matrix, $(B)_{kl} = \sum_{i,j=1}^{N} r_{jk} r_{il}\Phi(x_i - x_j)$ will decay as $|x_k - x_l|$ gets large.

Theorem 5.6. *Let Φ be the multiquadric and let $X = \{x_1, \dots, x_{N+1}\}$, $x_i = (\xi_i, \eta_i) \in \mathcal{R}^2$, be $N+1$ distinct points contained in the circle $|\cdot - x| \le H_1 < |x|$ where $x = x_{N+1}$. Also let $Y = \{y_1, \dots, y_{N+1}\}$, $y_i = (s_i, t_i) \in \mathcal{R}^2$, be $N+1$ distinct points contained in the circle $|\cdot| < H_2$ with $y_{N+1} = 0$. Then if $\beta \in \mathcal{U}_X$, $\gamma \in \mathcal{U}_Y$ and $|x| > H_1 + \sqrt{H_2^2 + c^2}$,*

$$\left| \sum_{i=1}^{N+1} \sum_{j=1}^{N+1} \gamma_i \beta_j \Phi(x_j - y_i) \right| \le \frac{20 H_1^2 H_2^2 E_1 E_2}{|x|^3} + \left| \mathcal{O}(|x|^{-4}) \right|,$$

where $E_1 = \sum_{i=1}^N |\beta_i|$ and $E_2 = \sum_{i=1}^N |\gamma_i|$. Furthermore, if β and γ are boundary over distance weights

$$\left| \sum_{i=1}^{N+1} \sum_{j=1}^{N+1} \gamma_i \beta_j \Phi(x_j - y_i) \right| \le \frac{640 Area(V_1) Area(V_2)}{|x|^3} + \left| \mathcal{O}(|x|^{-4}) \right|,$$

where V_1 is the Voronoi region around x_{N+1} and V_2 is the Voronoi region around y_{N+1}.

Proof. If $|x|$ is big enough we can approximate Φ by a far field expansion. For the multiquadric this was given by [3]. The far field expansion about zero for the multiquadrics $\Phi(\cdot - y_i)$ are valid for $|\cdot| > \sqrt{H_2^2 + c^2}$. Since by hypothesis $|x| > H_1 + \sqrt{H_2^2 + c^2}$ then $\min_{x \in X, y \in Y} |x - y| > \sqrt{H_2^2 + c^2}$. Now due to the sets X and Y being far enough apart, and

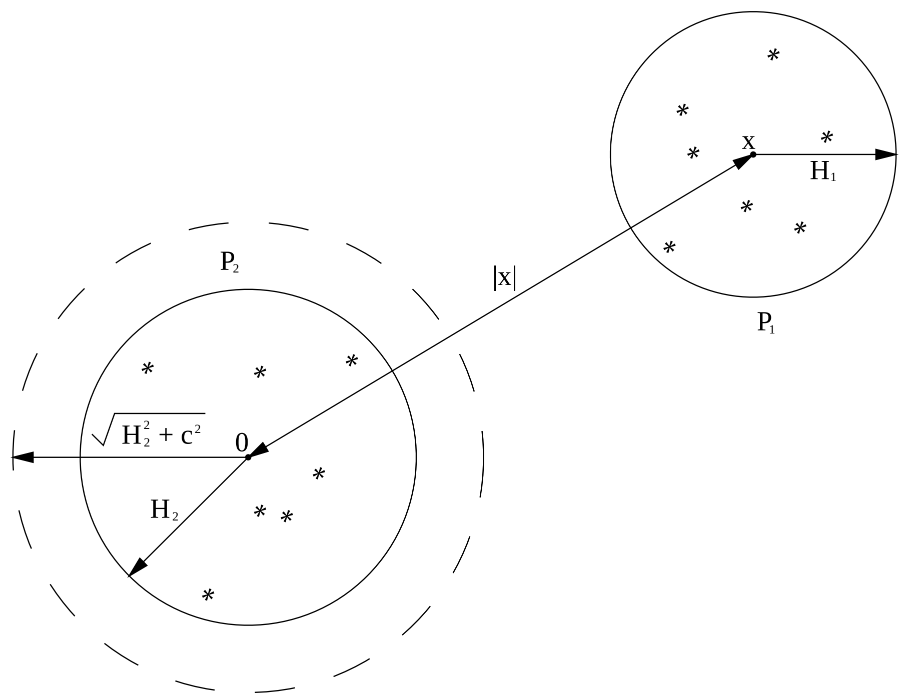

Figure 6: Two clusters of points (*) where the far field expansion is valid for any source point in P_1 and evaluation point in P_2.

because γ and β annihilate linears we obtain far field expansions of $\Phi(\cdot - y_i)$ about zero

$$\sum_{i,j=1}^{N+1} \gamma_i \beta_j \Phi(x_j - y_i) = \sum_{i,j=1}^{N+1} \gamma_i \beta_j \Bigg(|x_j| - \frac{s_i \xi_j + t_i \eta_j}{|x_j|} + \frac{1}{2} \frac{(t_i^2 + \tau^2)\xi_j^2 + (s_i^2 + \tau^2)\eta_j^2 - 2 s_i t_i \xi_j \eta_j}{|x_j|^3} + \mathcal{O}(|x|^{-2}) \Bigg),$$
$$= \sum_{i,j=1}^{N+1} \gamma_i \beta_j \left(\frac{1}{2} \frac{t_i^2 \xi_j^2 + s_i^2 \eta_j^2 - 2 s_i t_i \xi_j \eta_j}{|x_j|^3} + \mathcal{O}(|x|^{-2}) \right). \tag{30}$$

Taking absolute values and using Lemma 5.5 gives

$$\left| \sum_{i,j=1}^{N+1} \gamma_i \beta_j \Phi(x_j - y_i) \right| \leq \frac{20}{2} \frac{H_1^2 E_1}{|x|^3} \sum_{i=1}^{N+1} |\gamma_i| \Big(t_i^2 + s_i^2 + 2|s_i t_i| \Big) + \left| \mathcal{O}(|x|^{-4}) \right|,$$
$$\leq \frac{20 H_1^2 H_2^2 E_1 E_2}{|x|^3} + \left| \mathcal{O}(|x|^{-4}) \right|. \tag{31}$$

If β and γ are boundary over distance coefficients then

$$\left| \sum_{i,j=1}^{N+1} \gamma_i \beta_j \Phi(x_j - y_i) \right| \leq 40 \frac{\text{Area}(V_1)}{|x|^3} \sum_{i=1}^{N+1} |\gamma_i| \left(t_i^2 + s_i^2 + 2|s_i t_i| \right) + \left| \mathcal{O}(|x|^{-4}) \right|,$$
$$\leq 640 \frac{\text{Area}(V_1)\text{Area}(V_2)}{|x|^3} + \left| \mathcal{O}(|x|^{-4}) \right|. \tag{32}$$

□

Theorem 5.7. *Let Φ be the thin-plate spline and let $X = \{x_1, \ldots, x_{N+1}\}$, $x_i = (\xi_i, \eta_i) \in \mathcal{R}^2$, be $N+1$ distinct points contained in the circle $|\cdot - x| \leq H_1 < |x|$ where $x = x_{N+1}$. Also let $Y = \{y_1, \ldots, y_{N+1}\}$, $y_i = (s_i, t_i) \in \mathcal{R}^2$, be $N+1$ distinct points contained in the circle $|\cdot| < H_2$ with $y_{N+1} = 0$. Then if $\beta \in \mathcal{U}_X$, $\gamma \in \mathcal{U}_Y$ and $|x| > H_1 + H_2$,*

$$\left| \sum_{i=1}^{N+1} \sum_{j=1}^{N+1} \gamma_i \beta_j \Phi(x_j - y_i) \right| \leq \frac{44 H_1^2 H_2^2 E_1 E_2}{|x|^2} + \left| \mathcal{O}(|x|^{-3}) \right|,$$

where $E_1 = \sum_{i=1}^{N} |\beta_i|$ and $E_2 = \sum_{i=1}^{N} |\gamma_i|$. Furthermore, if β and γ are boundary over distance weights

$$\left| \sum_{i=1}^{N+1} \sum_{j=1}^{N+1} \gamma_i \beta_j \Phi(x_j - y_i) \right| \leq \frac{464 Area(V_1) Area(V_2)}{|x|^2} + \left| \mathcal{O}(|x|^{-3}) \right|,$$

where V_1 is the Voronoi region around x_{N+1} and V_2 is the Voronoi region around y_{N+1}.

Proof. With a similar approach to the proof of Theorem 5.6 we use the far field expansion of the thin-plate spline which is given in [4]. For $x = (\xi, \eta) > H_1 + H_2$ all the far field approximations will be valid. A single expansion of a thin-plate spline basic function centred at (s, t) is

$$\begin{aligned}
&\left[(\xi - s)^2 + (\eta - t)^2\right] \log\left(\left[(\xi - s)^2 + (\eta - t)^2\right]^{\frac{1}{2}}\right) \\
&= \frac{1}{2}(\xi^2 + \eta^2)\log(\xi^2 + \eta^2) - (s\xi + t\eta)\log(\xi^2 + \eta^2) - s\xi - t\eta \\
&\quad + \frac{1}{2}(s^2 + t^2)\log(\xi^2 + \eta^2) + \frac{1}{2}\frac{(3s^2 + t^2)\xi^2 + (s^2 + 3t^2)\eta^2 + 4st\xi\eta}{\xi^2 + \eta^2} + \mathcal{O}(|x|^{-1}).
\end{aligned} \tag{33}$$

Using this expansion and summing over the centres X and Y as in (30), the linear terms are annihilated giving

$$\begin{aligned}
\sum_{i,j=1}^{N+1} \gamma_i \beta_j \Phi(x_j - y_i) = \frac{1}{2}\sum_{i,j=1}^{N+1} \gamma_i \beta_j \Bigg(&(s_i^2 + t_i^2)\log(\xi_j^2 + \eta_j^2) \\
&+ \frac{(3s_i^2 + t_i^2)\xi_j^2 + (s_i^2 + 3t_i^2)\eta_j^2 + 4s_i t_i \xi_j \eta_j}{|x_j|^2} + \mathcal{O}(|x_j|^{-1})\Bigg).
\end{aligned} \tag{34}$$

A Taylor expansion of $\log(\xi_j^2 + \eta_j^2)$ about $x = (\xi, \eta)$ is

$$\begin{aligned}
\log(\xi_j^2 + \eta_j^2) = \log(\xi^2 + \eta^2) &- 2\frac{\xi\Delta\xi_j + \eta\Delta\eta_j}{|x|^2} \\
&+ \frac{\xi^2(\Delta\eta_j^2 - \Delta\xi_j^2) + \eta^2(\Delta\xi_j^2 - \Delta\eta_j^2) - 4\xi\eta\Delta\xi_j\Delta\eta_j}{|x|^4} + \mathcal{O}(|x|^{-3}).
\end{aligned} \tag{35}$$

Substituting this Taylor expansion into (34) and noticing that the first two terms in the Taylor expansion will be annihilated leads to the final summation

$$\begin{aligned}
&\sum_{i,j=1}^{N+1} \gamma_i \beta_j \Phi(x_j - y_i) \\
&\quad = \frac{1}{2}\sum_{i,j=1}^{N+1} \gamma_i \beta_j \Bigg((s_i^2 + t_i^2)\frac{\xi^2(\Delta\eta_j^2 - \Delta\xi_j^2) + \eta^2(\Delta\xi_j^2 - \Delta\eta_j^2) - 4\xi\eta\Delta\xi_j\Delta\eta_j}{|x|^4} \\
&\quad\quad + \frac{(3s_i^2 + t_i^2)\xi_j^2 + (s_i^2 + 3t_i^2)\eta_j^2 + 4s_i t_i \xi_j \eta_j}{|x_j|^2} + \mathcal{O}(|x_j|^{-1})\Bigg).
\end{aligned}$$

Taking absolute values and using Lemma 5.5 gives the result. □

The plots in Figure 7 show the distance $\|x_i - x_j\|$ vs $|B_{ij}|$ for a column j of B. The plotted values are only for indices i such that x_i is an internal centre. The total size of the data set is 400 centres of which 350 are internal. The decay rates mentioned in this section can easily be seen in the plots.

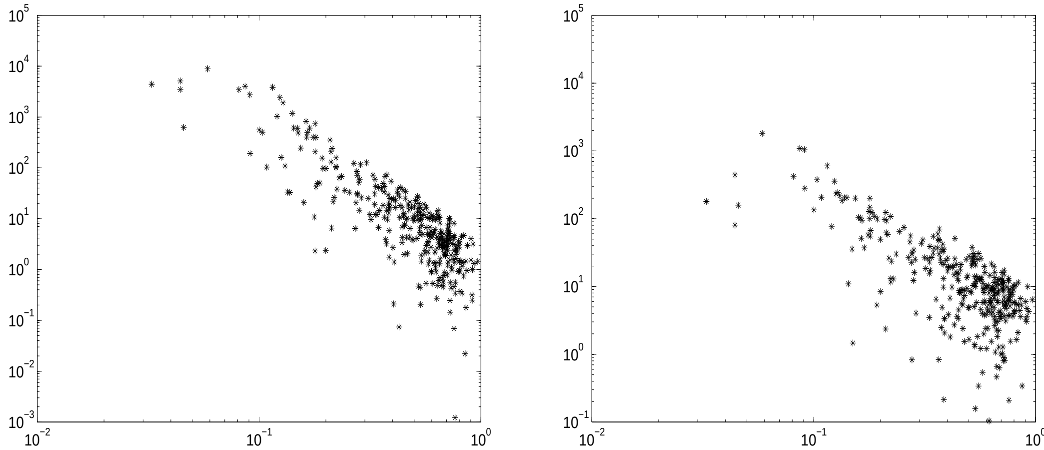

(a) Multiquadric basic function. (b) Thin-plate spline basic function.

Figure 7: Plots illustrating the results given in Theorems 5.6 and 5.7. The x-axis is $\|x_i - x_j\|$ and the y-axis is $|B_{ij}|$.

6 Numerical results

In this section we present numerical results for the following basic functions.

$$\text{thin-plate spline} \qquad \phi(r) = r^2 \log(r), \tag{36}$$

$$\text{linear} \qquad \phi(r) = -r, \tag{37}$$

$$\text{multiquadric} \qquad \phi(r) = -\sqrt{r^2 + c^2}, \tag{38}$$

$$\text{inverse multiquadric} \qquad \phi(r) = \frac{1}{\sqrt{r^2 + c^2}}. \tag{39}$$

Of these functions the thin-plate spline and linear functions satisfy the condition on Φ in Theorem 4.2 and will result in scale independent preconditioned matrices. In the following tables the matrix A_Φ is defined in (4), B in (5), S in Theorem 4.6 and the homogeneous matrix, C, is presented in [1]. In Table 1 we show condition numbers of matrices for the various preconditioning techniques over seven different scales. It is clear that the algorithm in Section 2 gives a matrix which dramatically improves the conditioning of the interpolation problem. In one case by a factor of 10^{14}! Tables 2–5 contain condition numbers of the matrices resulting from applying the preconditioning techniques of this paper for the basic functions (36)–(39). For $N < 3200$, the entries in the tables are the maximum over one hundred random point sets of size N. For $N = 3200$, the tables contain the maximum over twenty random point sets of size 3200. In all cases the preconditioning results in a smaller condition number. However the most impressive results are for the thin-plate spline, the linear, and the multiquadric basic functions. For these basic functions the maximum observed condition number of the scaled preconditioner, S, grows very slowly with N. Certainly there is no numerical evidence of power growth with N.

Scale parameter α	Conventional matrix A_ϕ	Homogeneous matrix C	Preconditioned matrix B	Scaled matrix S
0.001	1.531(11)	1.534(5)	4.905(1)	2.405(1)
0.01	1.544(9)	1.534(5)	4.905(1)	2.405(1)
0.1	1.597(7)	1.534(5)	4.905(1)	2.405(1)
1	3.107(5)	1.534(5)	4.905(1)	2.405(1)
10	1.915(6)	1.534(5)	4.905(1)	2.405(1)
100	1.271(11)	1.534(5)	4.905(1)	2.405(1)
1000	4.006(15)	1.534(5)	4.905(1)	2.405(1)

Table 1: Condition numbers for one hundred points in $[0,\ \alpha]^2$ and the thin-plate spline. The point set for scale α is , $X_\alpha = \alpha X_1$.

Number of data points	Conventional matrix A_ϕ	Homogeneous matrix C	Preconditioned matrix B	Scaled matrix S
100	1.852(7)	1.285(7)	3.865(2)	4.877(1)
200	6.555(7)	3.068(7)	1.617(3)	6.028(1)
400	5.675(8)	3.397(8)	1.945(3)	8.946(1)
800	1.960(10)	1.348(10)	2.034(3)	9.775(1)
1600	1.092(10)	8.413(9)	8.099(3)	1.258(2)
3200	4.997(10)	3.783(10)	1.261(4)	1.569(2)

Table 2: Maximum condition numbers encountered over a sample of 100 random point sets of size N in $[0,\ 1]^2$ with the thin-plate spline.

Number of data points	Conventional matrix A_ϕ	Preconditioned matrix B	Scaled matrix S
100	2.139(8)	1.129(2)	4.017(1)
200	2.014(8)	1.532(2)	4.224(1)
400	2.045(10)	5.932(2)	7.669(1)
800	6.641(10)	4.559(2)	5.826(1)
1600	1.554(10)	7.025(2)	5.601(1)
3200	2.477(11)	9.362(2)	6.280(1)

Table 3: Maximum condition numbers encountered over a sample of 100 random point sets of size N in $[0,\ 1]^2$ with the the multiquadric function with $c = 1/\sqrt{N}$.

Number of data points	Conventional matrix A_ϕ	Preconditioned matrix B	Scaled matrix S
100	9.732(4)	1.916(4)	6.468(1)
200	3.131(5)	6.099(4)	1.101(2)
400	1.178(6)	2.326(5)	2.364(2)
800	1.254(7)	2.826(5)	7.493(2)
1600	1.280(7)	4.227(5)	5.171(2)
3200	3.886(7)	2.815(6)	4.972(2)

Table 4: Maximum condition numbers encountered over a sample of 100 random point sets of size N in $[0,\ 1]^2$ with the linear function.

Number of data points	Conventional matrix A_ϕ	Preconditioned matrix B	Scaled matrix S
100	1.166(6)	1.180(3)	7.671(1)
200	9.370(5)	4.225(3)	1.725(2)
400	2.510(7)	9.017(3)	5.159(2)
800	5.853(7)	2.295(4)	1.338(3)
1600	8.174(6)	7.071(4)	3.633(3)
3200	5.311(7)	1.559(5)	9.997(3)

Table 5: Maximum condition numbers encountered over a sample of 100 random point sets of size N in $[0,\ 1]^2$ with the inverse multiquadric.

In an attempt to rule out the possibility that our numerical results were flukes due to the small number of 100 experiments we also conducted 50,000 trials with random data sets of size 100. The results of these trials are shown in Figure 1. The maximum condition number, over all trials with the thin-plate spline, for the matrix A_ϕ was 1.2465(9), for matrix C, 1.5750(9) and for matrix S, 1.8066(2). These maximum condition numbers and the results displayed in Figure 1 show that in our experiments the matrix S is always well conditioned. This held even for geometries of centres for which the matrix A_ϕ is very badly conditioned. These experiments lead one to suspect that the condition number of the matrix S may well be bounded independently of the geometry of the mesh. That is it may be bounded by a slowly growing function of N. To test further the behaviour of S for "bad" configurations of points a similar experiment was run with one thousand trials of one hundred points almost on a circle (for an example see Figure 8). The maximum condition numbers of the A matrix, C matrix and S matrix were 1.2885(9), 7.2692(8) and 6.6005(2) respectively over 1000 trials. Even though the Voronoi regions are long and thin the matrix is still well conditioned!

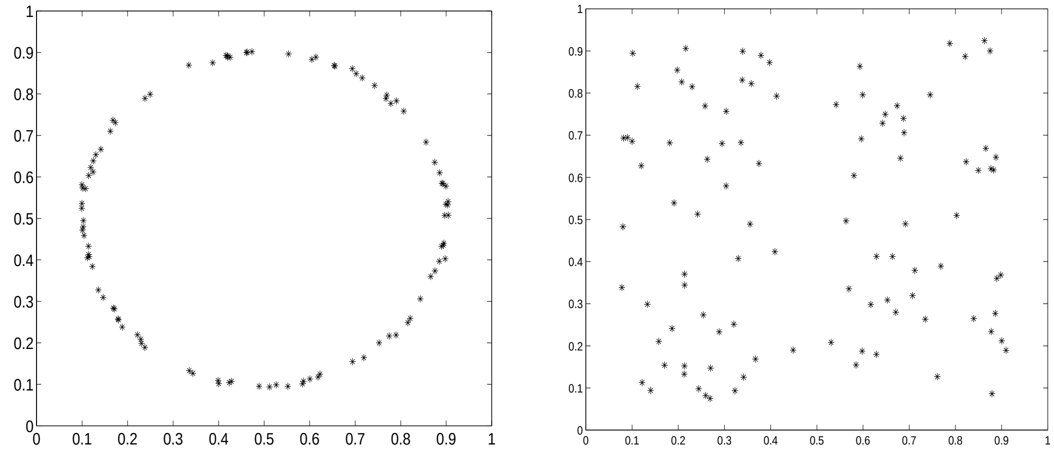

(a) One hundred centres almost on a cicle.

(b) One hundred random data points in the square.

Figure 8: Examples of two configurations of points in the domain $[0\ 1]^2$.

7 Preconditioning in $\mathcal{R}^3$

Common basic functions for RBF interpolation in $\mathcal{R}^3$ include the triharmonic $\Phi(\cdot) = |\cdot|^3$, the biharmonic $\Phi(\cdot) = |\cdot|$ and the multiquadric. The results of Narcowich and Ward show that for large data sets in $\mathcal{R}^3$ we would expect badly conditioned RBF interpolation matrices. Consequently there is a requirement for a preconditioner in three dimensions which reduces the condition number of the interpolation system. In this section we modify the algorithm of Section 2 in order to make it apply for this higher dimensional setting. It is not difficult to show that the theory in two dimensions can easily be transferred into three or more dimensions. For example in three dimensions, the coefficient matrix R, in Section 2 can be shown to be of rank $N-4$ and the invertibility of the preconditioned matrix follows.

One common form of surface fitting in $\mathcal{R}^3$ is the reconstruction of a closed surface, for example, a scanned object [5]. This can involve finding a zero surface and the centres are usually not uniformly distributed. More traditional interpolation is also required in three dimensions, for example, in meteorology or mining. The preconditioner of Section 2 can be modified and applied to both these cases. In the surface reconstruction case the Voronoi regions are often long and thin which may make it difficult for numerical techniques to accurately find the Voronoi vertices. This may lead to the columns of R not being completely orthogonal to the matrix Q.

One difference in three dimensions is that the boundary between two Voronoi regions is a face instead of a line. The corresponding boundary over distance weight is then given by the area of this face over the distance between the two centres. To write the virtual points uniquely as a homogeneous linear combination of special points we use four centres spread throughout the domain. The virtual points are then of the form

$$\hat{x}_j = \lambda_{N-3}x_{N-3} + \lambda_{N-2}x_{N-2} + \lambda_{N-1}x_{N-1} + \lambda_N x_N,$$

with $\lambda_{N-3} + \lambda_{N-2} + \lambda_{N-1} + \lambda_N = 1$. Implementing this algorithm in three dimensions is more complicated as centres with Voronoi regions adjacent to edges or corners can have up to three faces on the boundary (if the domain W is a cube) and therefore three virtual points. As before coefficients from each virtual point are added together. The complexity for finding the Voronoi regions in $\mathcal{R}^3$ is $\mathcal{O}(N^{4/3})$ operations so is slightly more expensive then the $\mathcal{O}(N \log N)$ operations in $\mathcal{R}^2$. Voronoi regions also have more neighbours in three dimensions and so slightly more work and storage is required to find the entries of R.

For uniformly distributed data in two dimensions the number of boundary points is $\mathcal{O}(N^{1/2})$ whereas in three dimensions this increases to $\mathcal{O}(N^{2/3})$. Consequently, more entries of B are sums of local centres and special points. The decay rates given in Theorems 5.6 and 5.7 for the two dimensional case are therefore valid for fewer entries in B. More simply put the preconditioner becomes less local which leads to the preconditioned matrix becoming less diagonally dominant and the eigenvalues less clustered. This is reflected in the condition numbers which are slightly higher than for the two dimensional case. However, as can be seen in Tables 6 - 8, they are still a great improvement over the usual formulation, A_Φ. For the multiquadric we see an improvement of almost six orders of magnitude between the condition number of A_Φ and the condition number of S for 3200 centres. When the triharmonic basic function or the biharmonic basic function are used the improvement is still significant.

Number of data points	Conventional matrix A_ϕ	Preconditioned matrix B	Scaled matrix S
100	9.9305(5)	9.8098(3)	1.6065(2)
200	9.1370(5)	1.3060(4)	2.5132(2)
400	1.1619(7)	3.5857(4)	4.0519(2)
800	4.3729(7)	5.3033(4)	7.4332(2)
1600	8.8497(7)	3.1376(5)	4.8450(2)
3200	5.5625(8)	1.6367(5)	8.7156(2)

Table 6: Condition numbers for various sized point sets in $[0,\ 1]^3$ for the multiquadric function, $c = 1/N^{1/3}$.

8 Roundoff error and fast computation of the action of the preconditioned matrix

In previous sections it has been shown that the preconditioned system B is much better conditioned than A. However, when N is large we cannot store B and therefore the matrix-

Number of data points	Conventional matrix A_ϕ	Preconditioned matrix B	Scaled matrix S
100	6.5877(5)	1.4062(4)	7.0990(2)
200	1.1382(6)	3.6882(4)	2.1499(3)
400	1.3393(7)	1.0986(5)	6.9424(3)
800	6.5861(7)	2.2407(5)	1.3153(4)
1600	2.4541(8)	1.3645(6)	3.0752(4)
3200	1.4898(9)	1.8674(6)	1.3097(5)

Table 7: Condition numbers for various sized point sets in $[0,\ 1]^3$ for the triharmonic function, $\Phi(\cdot) = |\cdot|^3$.

Number of data points	Conventional matrix A_ϕ	Preconditioned matrix B	Scaled matrix S
100	2.9886(3)	1.4888(2)	1.4788(1)
200	6.4223(3)	1.7203(2)	2.7998(1)
400	2.0965(4)	2.0112(2)	3.4539(1)
800	4.9875(4)	3.1780(2)	4.2342(1)
1600	1.6073(5)	4.9316(2)	6.1167(1)
3200	4.4444(5)	8.4780(2)	5.8858(1)

Table 8: Condition numbers for various sized point sets in $[0,\ 1]^3$ for the biharmonic function, $\Phi(\cdot) = |\cdot|$.

vector products that occur during an iterative fit are computed with a fast method and not by multiplying by B. In this section we address the question of whether this indirect approach somehow negates all the advantages of the preconditioning. The answer is that it need not, especially if one builds a fast evaluator for the preconditioned functions $\{\Psi_j\}$.

Since each ψ function is based on ϕ's corresponding to a local cluster of centres together with ϕ's associated with special points it is possible to develop hierarchical and fast multipole methods for fast approximate evaluation of $(AR)y$ rather than Ay. That is it is possible to construct fast evaluators which work with the ψ's rather than the ϕ's. The approximate computation of By during an iterative fit would then be performed as a two stage process, $t \approx (AR)y$ and $x = R^T t$. The question which naturally arises is will computing $x = By$ in this two stage manner give reliable estimates of x. A partial answer is given by the error analysis and tables below. These show that computing By in this two stage manner can be expected to be much less susceptible to roundoff than computing via the three stage process corresponding to a fast evaluator for ϕ, $v = Ry$, $w \approx Av$ and $x = R^T w$.

Let $B := R^T AR$ and x the exact product $x = By$. The finite precision counterpart is

$\hat{x} := fl(By)$ which from Higham [9, page 76] has error

$$\frac{\|\hat{x} - x\|}{\|x\|} \leq \alpha_N \|B\| \|B^{-1}\|, \tag{40}$$

where α_N is

$$\alpha_N = \frac{N\epsilon}{1 - N\epsilon},$$

with ϵ being the unit roundoff ($\approx 1 \times 10^{-16}$ for an IEEE double) and $\|\cdot\|$ is either the 1, ∞ or Frobenius norm.

Each column of R has a relatively small number, β say, of non-zero entries so the product $C = AR$ can be found accurately. From Higham [9, page 76], this matrix-matrix product will have error

$$\|C - \hat{C}\| \leq \alpha_\beta \|A\| \|R\|,$$

where $\hat{C} = fl(AR)$ is the finite precision product of AR. For large N, $\alpha_N \gg \alpha_\beta$ so for now we ignore the small error in finding C.

To find the product By by a two stage process without storing B requires the matrix-vector products,

$$t = Cy, \quad x = R^T t.$$

or in finite precision form,

$$\hat{x} = fl(R^T fl(Cy)).$$

We are interested in the error of computing $\hat{x}$. Let

$$\begin{aligned} \hat{t} &= fl(Cy), \\ &= (C + \Delta C)y, \quad |\Delta C| \leq \alpha_N |C|, \\ &= t + \Delta C y. \end{aligned}$$

Then $\hat{x}$ is

$$\begin{aligned} \hat{x} &= fl(R^T \hat{t}), \\ &= (R + \Delta R)^T \hat{t}, \quad |\Delta R| \leq \alpha_\beta |R|, \\ &= x + \Delta R^T t + R^T \Delta C y + \mathcal{O}(\epsilon^2). \end{aligned}$$

Paige [11] gives the relationship

$$\|\Delta R\| \leq \||\Delta R|\| \leq \alpha_\beta \||R|\| = \alpha_\beta \gamma_R \|R\|,$$

where $\gamma_R = 1$ if $\|\cdot\|$ is one of the 1, ∞ or Frobenius norms and $\gamma_R \leq \sqrt{n}$ for the 2-norm. A similar relationship exists between ΔC and C and between ΔA and A.

In the following discussion $\|\cdot\|$ is either the 2-norm or the Frobenius norm. The error in finding x is,

$$\begin{aligned}
\|\hat{x} - x\| &\leq \|\Delta R^T t\| + \|R^T \Delta C y\| + \mathcal{O}(\epsilon^2), \\
&\approx \|\Delta R^T C y\| + \|R^T \Delta C y\|, \\
&\leq \|\Delta R^T\| \|C\| \|y\| + \|R^T\| \|\Delta C\| \|y\|, \\
&\leq \alpha_\beta \gamma_R \|R\| \|C\| \|y\| + \alpha_N \gamma_C \|R\| \|C\| \|y\|, \\
&= (\alpha_\beta \gamma_R + \alpha_N \gamma_C) \|R\| \|C\| \|y\|.
\end{aligned}$$

Now $y = B^{-1}x$ implies $\|y\| \leq \|B^{-1}\| \|x\|$ which leads to the relative error

$$\frac{\|\hat{x} - x\|}{\|x\|} \lesssim \alpha_N \gamma_C \|B^{-1}\| \|R\| \|AR\| = \alpha_N b_2(X, \Phi), \tag{41}$$

where $b_2(X, \Phi) := \gamma_C \|B^{-1}\| \|R\| \|AR\|$. For the three stage process of finding $\hat{x}$ a similar analysis gives the bound

$$\frac{\|\hat{x} - x\|}{\|x\|} \lesssim \alpha_N \gamma_A \|B^{-1}\| \|R\|^2 \|A\| = \alpha_N b_3(X, \Phi), \tag{42}$$

with $b_3(X, \Phi) := \gamma_A \|B^{-1}\| \|R\|^2 \|A\|$. Note that the bounds given in this section are from a basic analysis and as such can be improved upon. However, they are acceptable here as they show that the two stage process, $x = R^T(Cy)$, will be sufficiently accurate for most purposes. Using the notation above, equation (40) for the 2-norm is

$$\frac{\|\hat{x} - x\|}{\|x\|} \leq \alpha_N \gamma_B \|B^{-1}\|_2 \|B\|_2 = \alpha_N b_1(X, \Phi), \tag{43}$$

where $b_1(X, \Phi) := \gamma_B \|B^{-1}\|_2 \|B\|_2$.

Tables 9-11 calculate the bounds (41) - (43) for various basic functions and centres, X, in $[0,\ 1]^2$. Numbers in the tables are with respect to the 2-norm. These results show that the bound on the two stage process is a lot smaller than the bound on the three stage process. As expected though direct multiplication with a stored B gives the smallest bound. Of course such direct multiplication is impractical for large N.

References

[1] R. K. Beatson, W. A. Light and S. Billings, Fast solution of the radial basis function interpolation equations: Domain decomposition methods, *SIAM Journal on Scientific Computing*, **22** (2000), 1717-1740.

[2] R. K. Beatson, J. B. Cherrie and C. T. Mouat, Fast fitting of radial basis functions: Methods based on preconditioned GMRES iteration, *Advances in Computational Mathematics*, **11** (1999), 253-270.

Grid size, N	$b_3(X, \Phi)$	$b_2(X, \Phi)$	$b_1(X, \Phi)$
10×10	5.928(4)	4.465(2)	3.285(1)
20×20	3.813(5)	8.258(2)	2.361(1)
30×30	1.663(6)	1.644(3)	2.401(1)
40×40	5.258(6)	2.919(3)	2.674(1)

Table 9: Bounds given in this section for the multiquadric basic function with $c = 1/N$.

[3] R. K. Beatson, J. B. Cherrie and G. N. Newsam, Fast evaluation of radial basis functions: Methods for generalised multiquadrics in $\mathcal{R}^n$. Manuscript (2001).

[4] R. K. Beatson and W. A. Light, Fast evaluation of radial basis functions: Methods for 2-dimensional polyharmonic splines, *IMA Journal of Numerical Analysis*, **17** (1997), 343-372.

[5] J. C. Carr, R. K. Beatson, J. B. Cherrie, T. J. Mitchell, W. R. Fright, B. C. McCallum and T. R. Evans, Reconstruction and representation of 3D objects with radial basis functions, to appear *SIGGRAPH 2001*, August 2001.

[6] N. H. Christ, R. Friedberg and T. D. Lee, Weights of links and plaquettes in a random lattice, *Nuclear Physics B* **210** (1982), 337-346.

[7] N. Dyn, D. Levin and S. Rippa, Numerical procedures for surface fitting of scattered data by radial functions, *SIAM Journal of Scientific and Statistical Computing*, **7** (1986), 639-659.

[8] J. Flusser, An adaptive method for image registration, *Pattern Recognition* **25** (1992), 45-54.

[9] N. J. Higham, *Accuracy and Stability of Numerical Algorithms*, Society for Industrial and Applied Mathematics, Philadelphia (1996).

[10] F. J. Narcowich and J. D. Ward, Norm estimates for the inverse of a general class of scattered-data radial-function interpolation matrices, *Journal of Approximation Theory*, **69** (1992), 84-109.

[11] C. C. Paige, Error analysis of the Lanczos algorithm for tridiagonalizing a symmetric matrix, *Journal of the Institute of Mathematics and its Applications*, **18** (1976), 341-349.

[12] R. Sibson and G. Stone, Computation of Thin-Plate Splines, *SIAM Journal on Scientific and Statistical Computing*, **12** (1991), 1304-1313.

Grid size, N	$b_3(X,\Phi)$	$b_2(X,\Phi)$	$b_1(X,\Phi)$
10×10	1.088(6)	6.685(3)	2.404(2)
20×20	7.140(6)	1.341(4)	2.248(2)
30×30	2.769(7)	2.464(4)	2.327(2)
40×40	7.068(7)	3.608(4)	2.130(2)

Table 10: Bounds given in this section for the multiquadric basic function with $c = 2/N$.

Grid size, N	$b_3(X,\Phi)$	$b_2(X,\Phi)$	$b_1(X,\Phi)$
10×10	2.053(4)	6.183(2)	3.328(1)
20×20	4.105(5)	2.946(3)	4.298(1)
30×30	2.260(6)	6.933(3)	4.308(1)
40×40	7.564(6)	1.263(4)	4.159(1)

Table 11: Bounds given in this section for the thin-plate spline basic function.

[13] G. Szego, *Orthogonal Polynomials*, American Math Society, Rhode Island (1978).

[14] R. S. Varga, *Matrix Iterative Analysis*, Prentice-Hall, New Jersey (1962).